

# XFT: Extending the Digital Application of the Fourier Transform

Rafael G. Campos<sup>(1)</sup>, J. Rico-Melgoza<sup>(2)</sup> and Edgar Chávez<sup>(1)</sup>

<sup>(1)</sup>Facultad de Ciencias Físico-Matemáticas,

<sup>(2)</sup>Facultad de Ingeniería Eléctrica

Universidad Michoacana,

58060, Morelia, Mich., México.

rcampos@umich.mx, jerico@umich.mx, elchavez@umich.mx

Keywords: Fractional Fourier Transform, Quadrature, Hermite polynomials, Fractional Discrete Fourier Transform, FFT

## Abstract

In recent years there has been a growing interest in the fractional Fourier transform driven by its great number of applications. The literature in this field follows two main routes. On the one hand the applications fields where the ordinary Fourier transform can be applied are being revisited to use this intermediate time-frequency representation of signals; and on the other hand fast algorithms for numerical computation of the fractional Fourier transform are devised. In this paper we derive a Gaussian-like quadrature of the continuous fractional Fourier transform. This quadrature is given in terms of the Hermite polynomials and their zeros. By using some asymptotic formulae we are able to solve the quadrature by a diagonal congruence transformation equivalent to a chirp-FFT-chirp transformation, yielding a fast discretization of the fractional Fourier transform and its inverse in closed form. We extend the range of the fractional Fourier transform by considering arbitrary complex values inside the unitary circle and not only at the boundary. Interestingly enough, the congruence transformation evaluated at  $z = i$ , which gives the Fourier transform, improves the standard discrete Fourier transform, yielding a new method to compute a more accurate FFT.

# 1 Introduction

A well-known fact is that the Fourier transform and some of its generalizations are frequently used tools in signal processing. The fractional Fourier transform [1, 2], which can be tracked down to the Wiener paper in 1929 [3] and is a particular case of the Linear Canonical Transform, which was derived in connection with canonical transformations in Quantum Mechanics [4, 5], has been object of renowned interest recently in the areas where the ordinary Fourier transform has been traditionally used. The work of Ozaktas et. al. [2] has established a standard framework to understand its properties and applications. The techniques known collectively as time-frequency or space-frequency analysis take advantage of the intermediate representation of the signal and its Fourier transform to give a richer representation. In almost any domain where the usual Fourier transform is used, there is room for techniques based on the space-frequency analysis. As examples we have the solution of differential equations, quantum optics, signal processing, swept frequency and time varying filters, pattern recognition and the study of time-frequency distributions [6]–[13]. Since this transform is a potentially useful tool for signal processing, the direct computation of the fractional Fourier transform in digital computers has become an important issue. In response to this need, an algorithm which computes a discrete fractional Fourier transform in  $\mathcal{O}(N \log N)$  time has been published [6].

In this paper a discrete fractional Fourier transform is obtained in a vector space of dimension  $N$  by using some properties of the Hermite polynomials. The finite-dimensional vectors representing a Hermite function and its Fourier transform converge to their exact continuous values when  $N$  goes to infinity, therefore, a matrix operator can be proposed as a representation of the kernel of the fractional Fourier transform for functions other than the Hermite ones. This matrix, which plays the role of the kernel, yields a quadrature formula [14, 15, 16] and a discrete form for the fractional Fourier transform. By using some asymptotic properties of the Hermite polynomials, this discrete fractional Fourier transform can be written in terms of the standard discrete Fourier transform through a diagonal congruence transformation. In this way, an efficient algorithm of  $\mathcal{O}(N \log N)$  complexity for fast computations of fractional Fourier transforms is obtained. To distinguish this discretization from other important contributions, particularly from those related with the discretization and development of fast algorithms to compute the linear canonical transformation [17, 18], it is called XFT (eXtended Fourier Transform). The XFT can be evaluated in closed form in terms of exponentials for any complex value  $z$  of the unit circle  $|z| \leq 1$ , though in the literature only values lying on the boundary  $|z| = 1$  are usually considered. Due to the diagonal congruence transformations, the XFT can be understood as a complex-windowed FFT.

## 2 Quadrature of the Fractional Fourier Transform

In this section, we reformulate the procedure followed in [14, 15, 16] to obtain a quadrature formula for the continuous fractional Fourier transform [1], yielding a discrete fractional Fourier transform, or as we call it, a **eXtended fast Fourier Transform**.

Let us consider the family of Hermite polynomials  $H_n(t)$ ,  $n = 0, 1, \dots$ , which satisfies the recurrence equation

$$H_{n+1}(t) + 2nH_{n-1}(t) = 2tH_n(t), \quad (1)$$

with  $H_{-1}(t) \equiv 0$ . As it is well-known [19], from (1) follows the Christoffel-Darboux formula [19]

$$\sum_{n=0}^{N-1} \frac{H_n(x)H_n(y)}{2^n n!} = \begin{cases} \frac{H_N(x)H_{N-1}(y) - H_{N-1}(x)H_N(y)}{2^N(N-1)!(x-y)}, & x \neq y, \\ \frac{H'_N(x)H_{N-1}(x) - H'_{N-1}(x)H_N(x)}{2^N(N-1)!}, & x = y. \end{cases} \quad (2)$$

Note that the recurrence equation (1) can be written as the eigenvalue problem

$$\begin{pmatrix} 0 & 1/2 & 0 & \cdots \\ 1 & 0 & 1/2 & \cdots \\ 0 & 2 & 0 & \cdots \\ \vdots & \vdots & \vdots & \ddots \end{pmatrix} \begin{pmatrix} H_0(t) \\ H_1(t) \\ H_2(t) \\ \vdots \end{pmatrix} = t \begin{pmatrix} H_0(t) \\ H_1(t) \\ H_2(t) \\ \vdots \end{pmatrix}. \quad (3)$$

Let us now consider the eigenproblem associated to the principal submatrix of dimension  $N$  of (3)

$$\mathcal{H} = \begin{pmatrix} 0 & 1/2 & 0 & \cdots & 0 & 0 \\ 1 & 0 & 1/2 & \cdots & 0 & 0 \\ 0 & 2 & 0 & \cdots & 0 & 0 \\ \vdots & \vdots & \vdots & \ddots & \vdots & \vdots \\ 0 & 0 & 0 & \cdots & 0 & 1/2 \\ 0 & 0 & 0 & \cdots & N-1 & 0 \end{pmatrix}.$$

This is a general technique [20, 21] to yield gaussian quadratures for orthogonal polynomials: the three-term recurrence equation is rewritten in matrix form to obtain orthonormal vectors of  $\mathbb{R}^N$  whose entries are given (in our case) in terms of the values of  $H_k(x)$ ,  $k = 0, 1, \dots, N-1$ , at the zeros of  $H_N(x)$ . We proceed by taking a similarity transformation to symmetrize  $\mathcal{H}$ . Note that the diagonal matrix given by

$$S = \text{diag} \left\{ 1, \frac{1}{\sqrt{2}}, \dots, \frac{1}{\sqrt{(N-1)! 2^{N-1}}} \right\},$$

generates the symmetric matrix

$$H = S\mathcal{H}S^{-1} = \begin{pmatrix} 0 & \sqrt{\frac{1}{2}} & 0 & \cdots & 0 & 0 \\ \sqrt{\frac{1}{2}} & 0 & \sqrt{\frac{2}{2}} & \cdots & 0 & 0 \\ 0 & \sqrt{\frac{2}{2}} & 0 & \cdots & 0 & 0 \\ \vdots & \vdots & \vdots & \ddots & \vdots & \vdots \\ 0 & 0 & 0 & \cdots & 0 & \sqrt{\frac{N-1}{2}} \\ 0 & 0 & 0 & \cdots & \sqrt{\frac{N-1}{2}} & 0 \end{pmatrix}.$$

The recurrence equation (1) and formula (2) can be used to solve the eigenproblem

$$Hu_k = t_k u_k, \quad k = 1, 2, \dots, N,$$

which is a finite-dimensional version of (3). The eigenvalues  $t_k$  are the zeros of  $H_N(t)$  and the  $k$ th eigenvector  $u_k$  is given by

$$c_k (s_1 H_0(t_k), s_2 H_1(t_k), s_3 H_2(t_k), \dots, s_N H_{N-1}(t_k))^T,$$

where  $s_1, \dots, s_N$  are the diagonal elements of  $S$  and  $c_k$  is a normalization constant that can be determined from the condition  $u_k^T u_k = 1$ , i.e., from

$$c_k^2 \sum_{n=0}^{N-1} \frac{H_n(t_k) H_n(t_k)}{2^n n!} = 1.$$

Since  $H_N(t_k) = 0$  and  $H'_N(t_k) = 2N H_{N-1}(t_k)$ , the use of (2) yields

$$c_k = \sqrt{\frac{2^{N-1} (N-1)!}{N}} \frac{1}{|H_{N-1}(t_k)|} = \sqrt{\frac{2^{N-1} (N-1)!}{N}} \frac{(-1)^{N+k}}{H_{N-1}(t_k)},$$

where we have used the fact that  $|H_{N-1}(t_k)| = (-1)^{N+k} H_{N-1}(t_k)$ . Thus, the components of the orthonormal vectors  $u_k$ ,  $k = 1, 2, \dots, N$ , are

$$(u_k)_n = (-1)^{N+k} \sqrt{\frac{2^{N-n} (N-1)!}{N (n-1)!}} \frac{H_{n-1}(t_k)}{H_{N-1}(t_k)}, \quad n = 1, \dots, N. \quad (4)$$

Let  $U$  be the orthogonal matrix whose  $k$ th column is  $u_k$  and  $D(z)$  be the diagonal matrix  $D(z) = \text{diag}\{1, z, z^2, \dots, z^{N-1}\}$ , where  $z$  is a complex number. Now, let us define the matrix

$$\mathcal{F}_z = \sqrt{2\pi} U^{-1} D(z) U$$

whose components are given by

$$(\mathcal{F}_z)_{jk} = \sqrt{2\pi} \frac{(-1)^{j+k} 2^{N-1} (N-1)!}{N H_{N-1}(t_j) H_{N-1}(t_k)} \sum_{n=0}^{N-1} \frac{z^n}{2^n n!} H_n(t_j) H_n(t_k). \quad (5)$$

This is the matrix representing the kernel of the fractional Fourier transform in a  $N$ -dimensional vector space, as we show next.

## Asymptotic formulae

Let us look for the asymptotic form of the components (5) of  $\mathcal{F}_z$ . First note that the asymptotic expression for  $H_N(t)$  in the oscillatory region is (Eq. (8.22.8) of [19])

$$H_N(t) = \frac{\Gamma(N+1)}{\Gamma(N/2+1)} e^{t^2/2} \left( \cos(\sqrt{2N+1} t - N\pi/2) + \mathcal{O}(N^{-1/2}) \right). \quad (6)$$

This gives an approximate form for the zeros of  $H_N(t)$ , i.e.,

$$t_k \simeq \left( \frac{2k - N - 1}{\sqrt{2N}} \right) \frac{\pi}{2}, \quad (7)$$

$k = 1, 2, \dots, N$ . Thus, the use of (6) and (7) yields

$$H_{N-1}(t_k) \simeq (-1)^{N+k} \frac{\Gamma(N)}{\Gamma(\frac{N+1}{2})} e^{t_k^2/2}, \quad N \rightarrow \infty.$$

Therefore, for  $N$  great enough, (5) can be written as

$$(\mathcal{F}_z)_{jk} \simeq \sqrt{2\pi} \frac{2^{N-1} [\Gamma(\frac{N+1}{2})]^2}{\Gamma(N+1)} e^{-(t_j^2+t_k^2)/2} \sum_{n=0}^{\infty} \frac{z^n}{2^n n!} H_n(t_j) H_n(t_k),$$

and finally, Stirling's formula and Mehler's formula [22] produce the result

$$(\mathcal{F}_z)_{jk} \simeq \sqrt{\frac{2}{1-z^2}} \exp \left( -\frac{(1+z^2)(t_j^2+t_k^2) - 4t_j t_k z}{2(1-z^2)} \right) \Delta t_k, \quad (8)$$

where  $\Delta t_k$  is the difference between two consecutive asymptotic Hermite zeros, i.e.,

$$\Delta t_k = t_{k+1} - t_k = \frac{\pi}{\sqrt{2N}}. \quad (9)$$

Let us consider now a complex-valued function  $g(t)$  defined for  $t \in \mathbb{R}$  and let us form the vector

$$g = (g(t_1), g(t_2), \dots, g(t_N))^T.$$

Therefore, the multiplication of the matrix  $\mathcal{F}_z$  by the vector  $g$  gives the vector  $G$  with entries

$$G_j = \sum_{k=1}^N (\mathcal{F}_z)_{jk} g(t_k) \simeq \sqrt{\frac{2}{1-z^2}} \sum_{k=1}^N \exp \left( -\frac{(1+z^2)(t_j^2+t_k^2) - 4t_j t_k z}{2(1-z^2)} \right) g(t_k) \Delta t_k, \quad (10)$$

for  $j = 1, 2, \dots, N$ . Note that this equation is a Riemann sum for the integral

$$\mathcal{F}_z[g(t'), t] = \sqrt{\frac{2}{1-z^2}} \int_{-\infty}^{\infty} \exp \left( -\frac{(1+z^2)(t^2+t'^2) - 4t t' z}{2(1-z^2)} \right) g(t') dt', \quad |z| < 1, \quad (11)$$

that is,

$$\mathcal{F}_z[g(t'), t_j] \simeq \sum_{k=1}^N (\mathcal{F}_z)_{jk} g(t_k), \quad N \rightarrow \infty. \quad (12)$$

Note that  $\mathcal{F}_z[g(t'), t]$  is the continuous fractional Fourier transform [1] of  $g(t')$  up to a constant. Thus, the matrix  $\mathcal{F}_z$  is a discrete fractional Fourier transform. Since the fractional transform is an extension for the Fourier transform,  $\mathcal{F}_z$  is termed XFT. It should be noted that the XFT is a discretization of the fractional Fourier transform for any complex value  $z$  of the unitary circle  $|z| \leq 1$  and not only for  $z$  lying on its boundary, as it is usually considered. Note that for the XFT, the argument  $\varphi$  of  $z = r \exp(i\varphi)$  is real and not complex as it is used in some applications [23].

In the case  $z = \pm i$ , (8) becomes

$$F_{jk} \equiv (\mathcal{F}_{\pm i})_{jk} \simeq e^{\pm i t_j t_k} \Delta t_k,$$

that is, the XFT becomes a discrete Fourier transform. It has been previously obtained in [14] where some numerical examples are given, and it has been applied to the analysis of brain signals [24].

### 3 The fast XFT

The FFT can be used to obtain a fast algorithm for the XFT as following. Since the matrix  $\mathcal{F}_z$  represents a quadrature for the fractional Fourier transform expected to converge when a great number of nodes are used, we consider the asymptotic form (8) which can be written in more detail as

$$(\mathcal{F}_z)_{jk} = \sqrt{\frac{2}{1-z^2}} \exp(-\mu t_j^2) \exp(\nu t_j t_k) \exp(-\mu t_k^2) \Delta t_k, \quad (13)$$

where we have used the definitions

$$\mu = \frac{1+z^2}{2(1-z^2)}, \quad \nu = \frac{2z}{1-z^2}. \quad (14)$$

Note that we have replaced the approximately equal sign " $\simeq$ " by the equal sign " $=$ " in (13) redefining  $\mathcal{F}_z$ . In order to show the main differences of the XFT with the usual FFT, we consider first the case of the standard Fourier transform.

#### 3.1 XFT as an improvement of the FFT

As noted above, the case  $z = i$  in (13) corresponds to a discrete Fourier transform

$$F_{jk} = \frac{\pi}{\sqrt{2N}} \exp \left[ i \frac{\pi^2}{2N} \left( j - \frac{N-1}{2} \right) \left( k - \frac{N-1}{2} \right) \right] \quad (15)$$

where now  $j, k = 0, 1, 2, \dots, N-1$ , and we have used (7) and (9). Since  $\sum_{k=1}^N F_{jk}g(t_k)$  is a quadrature and therefore, an approximation [cf. Eq. 12] of

$$G(\omega_j) = \int_{-\infty}^{\infty} e^{i\omega_j t} g(t) dt,$$

we can use the basic property of the Fourier transform

$$G(a\omega_j) = \int_{-\infty}^{\infty} e^{ia\omega_j t} g(t) dt \quad (16)$$

to rewrite (15) in the more convenient form

$$(F_a)_{jk} = \frac{\pi}{\sqrt{2N}} \exp \left[ ia \frac{\pi^2}{2N} \left( j - \frac{N-1}{2} \right) \left( k - \frac{N-1}{2} \right) \right], \quad (17)$$

in the understanding that this matrix yields a scaled Fourier transform. If we choose  $a = 4/\pi$ , Eq. (17) can be written as

$$(F_{4/\pi})_{jk} = \frac{\pi e^{i\frac{\pi}{2}\frac{(N-1)^2}{N}}}{\sqrt{2N}} \left[ e^{-i\pi\frac{N-1}{N}j} \right] \left[ e^{i\frac{2\pi}{N}jk} \right] \left[ e^{-i\pi\frac{N-1}{N}k} \right],$$

where  $j, k = 0, 1, 2, \dots, N-1$ . In matrix form, and defining  $\tilde{F} \equiv F_{4/\pi}$  to simplify the notation,

$$\tilde{F} = \frac{\pi e^{i\frac{\pi}{2}\frac{(N-1)^2}{N}}}{\sqrt{2N}} S D_F S, \quad (18)$$

where  $S$  is the diagonal matrix whose nonzero elements are  $\exp(-i\pi(N-1)j/N)$ ,  $j = 0, 1, \dots, N-1$  and  $D_F(\cdot)$  is just the FFT of the argument.

Note that a very important contribution of our result is that it truly enables the extension of the FFT algorithms to a more general case. The fact that computing  $\tilde{F}(\cdot)$  is essentially computing the FFT of the vector  $S(\cdot)$ , means that almost at no cost, modern instruments would be able to increase their capabilities for digital processing.

The inverse of  $\tilde{F}$  is easily obtained:

$$(\tilde{F}^{-1})_{jk} = \frac{\sqrt{2/N}}{\pi} \exp \left[ -i\frac{2\pi}{N} \left( j - \frac{N-1}{2} \right) \left( k - \frac{N-1}{2} \right) \right],$$

where  $j, k = 0, 1, 2, \dots, N-1$ .

In the applications, we have to remind that  $\tilde{F}$  gives a scaled transform. The following simple algorithm incorporate these ideas.

### Algorithm 1

To compute an approximation  $G = (G_1, G_2, \dots, G_N)^T$  of the Fourier transform (16) of the vector

$$g = (g_1, g_2, \dots, g_N)^T.$$

1. For  $j, k = 0, 1, 2, \dots, N - 1$ ,
  - (a) Compute  $(D_F)_{jk} = e^{i\frac{2\pi}{N}jk}$  (the discrete Fourier transform).
  - (b) Compute the diagonal matrix  $S$  according to  $S_{jk} = e^{-i\pi\frac{N-1}{N}j}\delta_{jk}$ .
2. Obtain the approximation  $G_j$  to  $G(\frac{4}{\pi}t_j)$  by computing the matrix-vector product

$$G = \frac{\pi e^{i\frac{\pi}{2}\frac{(N-1)^2}{N}}}{\sqrt{2N}} S D_F (Sg), \quad (19)$$

with a standard FFT algorithm.

Either if the input vector  $g$  is given by the values of a function  $g(t)$  at  $t_k$ , or not, we can represent the approximation to the Fourier transform  $G(\omega)$ , as given in a plot of points  $(\frac{4}{\pi}t_j, G_j)$ .

In the examples given below we plot the real and imaginary parts of the vector  $G$  and the exact transform  $G(\frac{4}{\pi}\omega)$ . We give first two examples of non-periodic/singular functions [25]. To compare the performance of XFT with that of FFT, we show the plot of the corresponding FFT in the first example.

### Example 1

Consider the pair of Fourier transforms

$$g(t) = \cos(t^2), \quad G(\omega) = \sqrt{\pi} \cos\left(\frac{\omega^2 - \pi}{4}\right).$$

Figures 1 and 2 shows the numerical convergence attained by the XFT for  $N=512$  and 1024 respectively and it is compared with the FFT output.



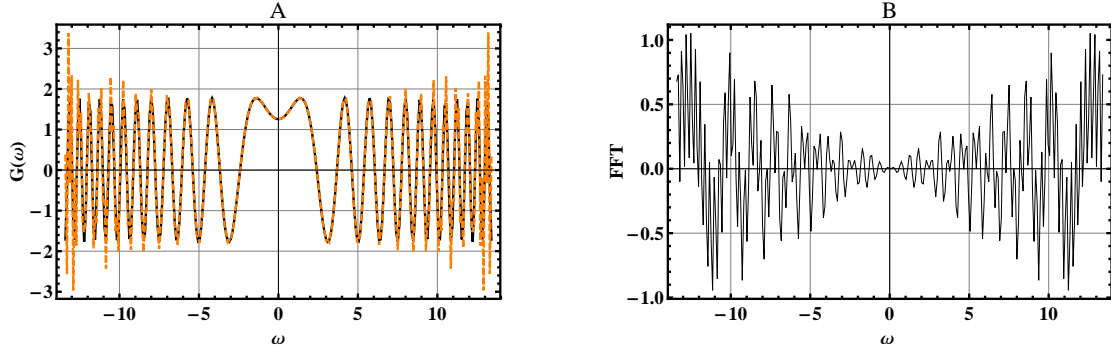


Figure 1: **A** Part of the plots corresponding to  $(t_j, G(\frac{4}{\pi}t_j))$  (solid line) and  $(t_j, G_j)$  (dashed line). The max-norm of the overall error is 2.11 for  $N = 512$ . **B** The standard FFT computed for the same function and number of points.

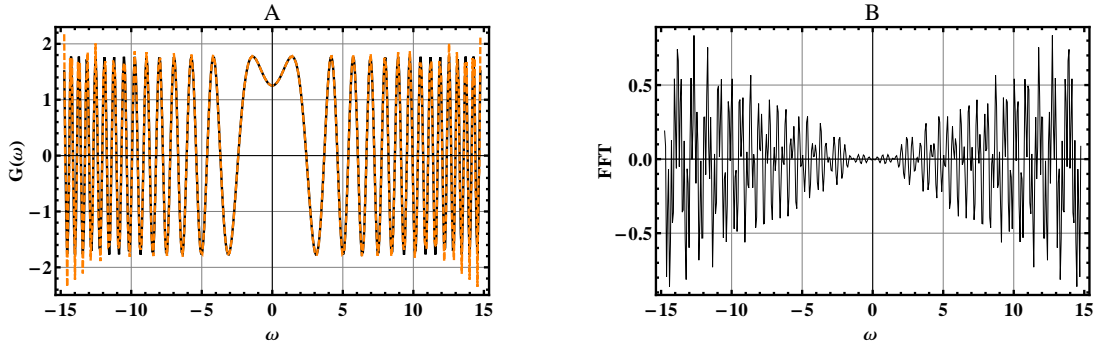


Figure 2: **A** Part of the plots corresponding to  $(t_j, G(\frac{4}{\pi}t_j))$  (solid line) and  $(t_j, G_j)$  (dashed line). The max-norm of the overall error is 2.08 for  $N = 1024$ . **B** The standard FFT computed for the same function and number of points.

## Example 2

As an example of a singular function, let us consider the pair of Fourier transforms (the integral is a Cauchy Principal Value)

$$g(t) = \frac{e^{-t/2}}{b - e^{-t}}, \quad b > 0, \quad G(\omega) = \frac{\pi}{b^{1/2+i\omega}} \cot\left(\frac{\pi}{2} - i\pi\omega\right).$$

Figures 3 and 4 shows the good performance of the XFT for  $N=512$  and  $1024$  respectively. In this cases we have small absolute errors.

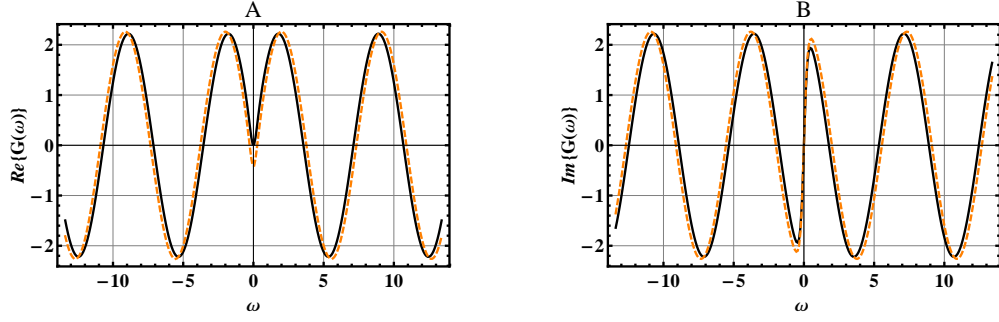


Figure 3: **A** Real part and **B** imaginary part of the continuous Fourier transform (solid line) compared with the XFT (dashed line) computed with  $N = 512$ . The function  $f(t)$  is that given in Example 2. The max-norm of the overall error is 0.4262 for both the real and imaginary part.

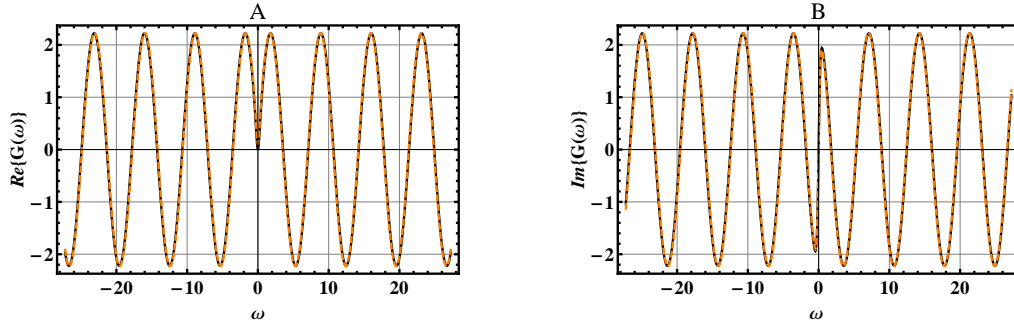


Figure 4: **A** Real part and **B** imaginary part of the continuous Fourier transform (solid line) compared with the XFT (dashed line) computed with  $N = 1024$ . The function  $f(t)$  is that given in Example 2. The max-norm of the overall error is 0.105 for both the real and imaginary part.

### Example 3

This example is concerned with the performance of the XFT acting on sinusoidal waveforms of integer-harmonic frequency. Our starting point is again Eq. (17). By changing the order of the indexes, (17) can be written as

$$(\tilde{F})_{jk} = \frac{\pi}{\sqrt{2N}} e^{i \frac{2\pi}{N} jk},$$

where

$$j, k = \begin{cases} 0, \pm 1, \pm 2, \dots, \pm(N-1)/2, & N \text{ odd}, \\ \pm 1/2, \pm 3/2, \dots, \pm(N-1)/2, & N \text{ even}. \end{cases}$$

Let  $N$  be odd, and assume that the signal to be transformed is an integer-harmonic signal. For instance,

$$g_k = \cos(k\tau_m), \quad \tau_m = \frac{2\pi m}{N}, \quad (20)$$

where  $k = 0, \pm 1, \pm 2, \dots, \pm(N-1)/2$ . Then, the formulae [26]

$$\sum_{k=1}^N \cos(kx) = \frac{\sin(Nx/2) \cos((N+1)x/2)}{\sin(x/2)}, \quad \sum_{k=1}^N \sin(kx) = \frac{\sin(Nx/2) \sin((N+1)x/2)}{\sin(x/2)},$$

can be used to prove that the XFT transform of (20) is

$$G_j = \sum_{k=-(N-1)/2}^{(N-1)/2} (\tilde{F})_{jk} \cos(k\tau_m) = \pi \sqrt{\frac{N}{2}} (\delta_{j,-m} + \delta_{jm}), \quad (21)$$

where  $j = 0, \pm 1, \pm 2, \dots, \pm(N-1)/2$ , corresponding to two pulses centered at the integers  $m$  and  $-m$  respectively.

Now assume that  $N$  is even and take a half-integer harmonic signal, i.e., one of the same form as (20) but with  $k = \pm 1/2, \pm 3/2, \dots, \pm(N-1)/2$ . A similar calculation as above shows that  $G_j$  has the same form of (21) but the sum runs over half-integers and the pulses are now centered at the half-integers  $m$  and  $-m$  respectively.

In the two above cases the dispersion is zero, but this does not happen if we take  $N$  odd and consider a half-integer harmonic signal, or  $N$  even and consider an integer harmonic signal. Finally note that these processes can be reversed: the XFT of the corresponding pulses yields integer or half-integer harmonic signals.

We give another numerical case with a cosine waveform with an arbitrary frequency. Let us consider the example  $g(t) = \cos(5.156t)$ . In Fig. 5 we show the XFT output for (a)  $N = 1024$  and (b)  $N = 2048$ . As it can be seen, the leakage practically vanishes for the latter case. As a measure of the leakage we give the mean value

$$\mu = \frac{1}{N} \sum_{k=1}^N (|G_k| - \delta_{km}|G_m| - \delta_{km'}|G_{m'}|),$$

where the indexes  $m$  and  $m'$  correspond to the frequencies where  $|G|$  attains their maxima. Thus, we find that  $\mu = 0.14105$  for  $N = 1024$  and  $\mu = 0.00276$  for  $N = 2048$ .

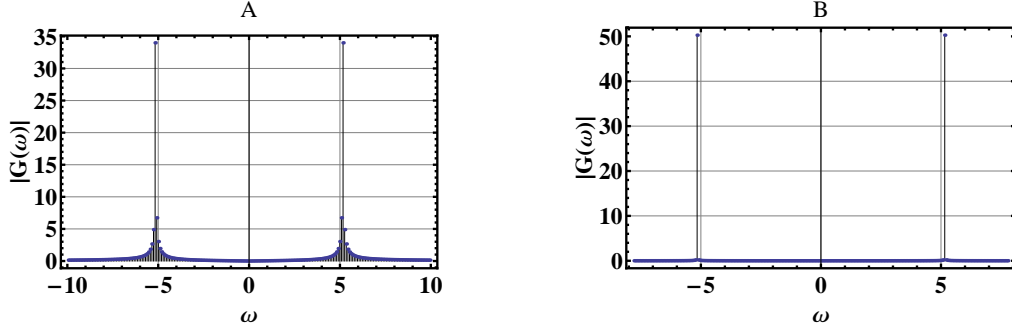


Figure 5: Fourier transform of  $\cos(5.156 t)$ . The maximum occurs at  $\omega = 5.17072$  for **A**  $N = 1024$  and at  $\omega = 5.15625$  for **B**  $N = 2048$ .

### 3.2 XFT as a fast discrete fractional Fourier transform

To obtain a discrete and fast implementation of the continuous fractional Fourier transform, we follow the same procedure as above. The definition of the fractional transform given by (11) is  $\sqrt{2\pi}$  times the one given in [1]. This has to be taken into account for comparing purposes.

Our starting point is the definition of the fractional transform given in (11)

$$G_z(t) \equiv \mathcal{F}_z[g(t'), t] = \sqrt{\frac{2}{1-z^2}} e^{-\mu t^2} \int_{-\infty}^{\infty} e^{\nu t t'} e^{-\mu t'^2} g(t') dt',$$

where we have used the definitions (14). The simple scaling

$$G_z(at) = \sqrt{\frac{2}{1-z^2}} e^{-\mu a^2 t^2} \int_{-\infty}^{\infty} e^{a \nu t t'} e^{-\mu t'^2} g(t') dt', \quad (22)$$

and the discretization of the kernel

$$(\mathcal{F}_z^a)_{jk} = \sqrt{\frac{2}{1-z^2}} \exp(-\mu a^2 t_j^2) \exp(a \nu t_j t_k) \exp(-\mu t_k^2) \Delta t_k,$$

allows us to implement a fast algorithm to compute the XFT in terms of the FFT. This can be done by choosing  $a = i2(1-z^2)/(\pi z)$ , because then

$$(\mathcal{F}_z^a)_{jk} = \sqrt{\frac{2}{1-z^2}} \exp(-\mu a^2 t_j^2) (\tilde{F})_{jk} \exp(-\mu t_k^2), \quad a = \frac{2i}{\pi z}(1-z^2),$$

where  $\tilde{F}$ , given by (18), is the fast XFT for the case of the standard Fourier transform. In order to simplify the notation, let  $\tilde{\mathcal{F}}_z$  be  $\mathcal{F}_z^{2i(1-z^2)/(\pi z)}$ . Since  $\sum_{k=1}^N (\tilde{\mathcal{F}}_z)_{jk} f(t_k)$  is a quadrature of (22) with  $a = i2(1-z^2)/(\pi z)$  [cf. Eq. 12],  $\tilde{\mathcal{F}}_z$  is a fast discrete fractional

Fourier transform which gives an approximation for the scaled function  $G_z(at)$  at the nodes  $t_k$ . Note that the inverse transform can be obtained in terms of  $\tilde{F}^{-1}$ . These ideas are incorporated in the following

Algorithm 2

To compute an approximation  $G_z = (G_{z1}, G_{z2}, \dots, G_{zN})^T$  of the fractional Fourier transform  $\mathcal{F}_z[g(t'), i2(1 - z^2)/(\pi z)t_j]$  of the vector

$$g = (g_1, g_2, \dots, g_N)^T,$$

at the complex value  $z$ ,  $|z| \leq 1$ .

1. For given  $N$  and  $z$ , set

(a)  $\mu = (1 + z^2)/[2(1 - z^2)], \quad a = 2i(1 - z^2)/(\pi z).$

(b)  $t_k = \pi(2k - N - 1)/[2(\sqrt{2N})], \quad k = 1, 2, \dots, N$

2. For  $j, k = 0, 1, 2, \dots, N - 1$ ,

(a) Compute  $(D_F)_{jk} = e^{i\frac{2\pi}{N}jk}$  (the discrete Fourier transform).

(b) Compute the diagonal matrices  $S_1$  and  $S_2$  according to

$$(S_1)_{jk} = e^{-\mu a^2 t_j^2 - i\pi \frac{N-1}{N} j} \delta_{jk}, \quad (S_2)_{jk} = e^{-\mu t_j^2 - i\pi \frac{N-1}{N} j} \delta_{jk}.$$

3. Obtain the approximation  $G_{zj}$  to  $G_z(\frac{4}{\pi}t_j)$  by computing the matrix-vector product

$$G_z = \sqrt{\frac{2}{1 - z^2}} \frac{\pi e^{i\frac{\pi}{2} \frac{(N-1)^2}{N}}}{\sqrt{2N}} S_1 D_F (S_2 g), \quad (23)$$

with a standard FFT algorithm.

We first test this fast transform on two well-known examples for which  $|z| = 1$  (see Ref. [1]).

#### Example 4

Consider the pair of fractional Fourier transforms

$$g(t) = \exp(-t^2/2 + \beta t), \quad G_z(t) = \exp(-t^2/2 - (i/2)\beta^2 e^{i\varphi} \sin \varphi + \beta t e^{i\varphi}), \quad z = e^{i\varphi}.$$

Fig. 6 shows a part of the plot of the real and imaginary parts of the XFT compared with  $G_z(at_j)$  for this case. The max-norm of the error is of order  $10^{-12}$  for both cases.

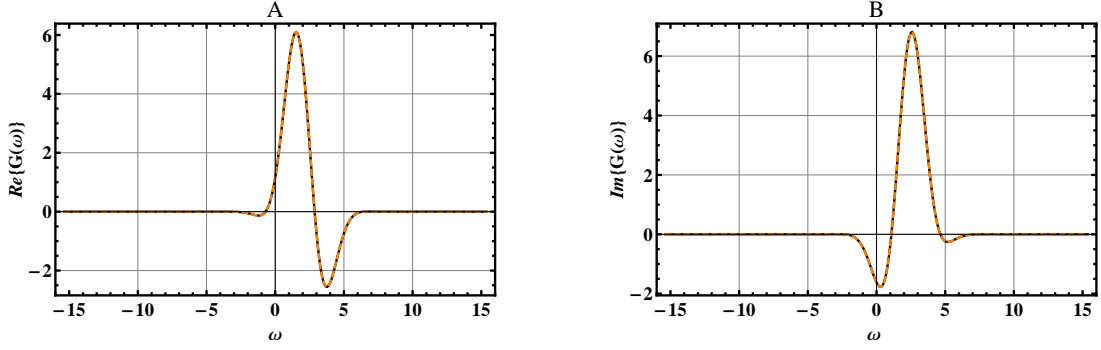


Figure 6: **A** Real part and **B** imaginary part of the fractional Fourier transform (solid line) compared with the XFT (dashed line) computed with  $N = 512$ . The function  $f(t)$  is that given in Example 4 for  $\beta = 2$ .

### Example 5

Consider the pair of fractional Fourier transforms

$$g(t) = 1, \quad G_z(t) = \exp[i(t^2 \tan \varphi - \varphi)/2] / \sqrt{\cos \varphi}, \quad z = e^{i\varphi}.$$

Fig. 7 shows the whole plot of the real and imaginary parts of the XFT compared with  $G_z(at_j)$  for this case. The max-norm of the overall error is 1.3282 for the real part and 1.42694 for the imaginary part.

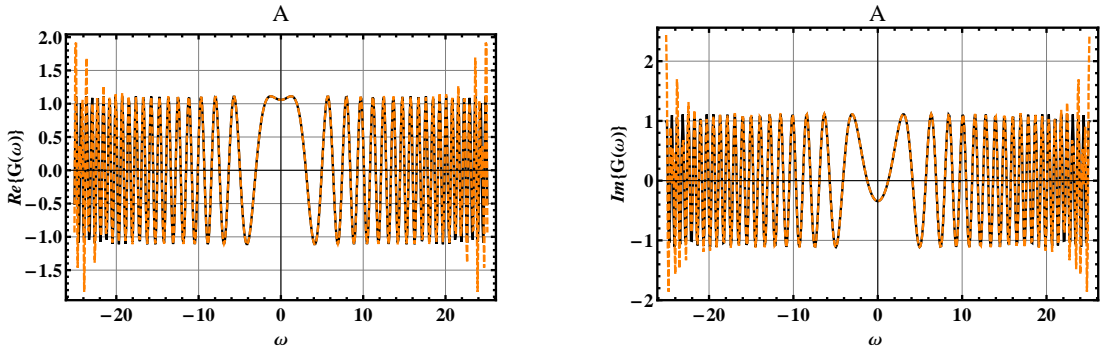


Figure 7: **A** Real part and **B** imaginary part of the fractional Fourier transform (solid line) compared with the XFT (dashed line) computed with  $N = 512$ . The function  $f(t)$  is that given in Example 5.

### Example 6

This example consider the fractional Fourier transform of the rectangle function. The cases correspond to the fractional Fourier transform as defined in the literature [1], for the values of the argument  $\varphi$  given in the caption. This figure shows how the Fourier transform evolves as the argument of  $z = \exp(i\varphi)$  takes decreasing values.

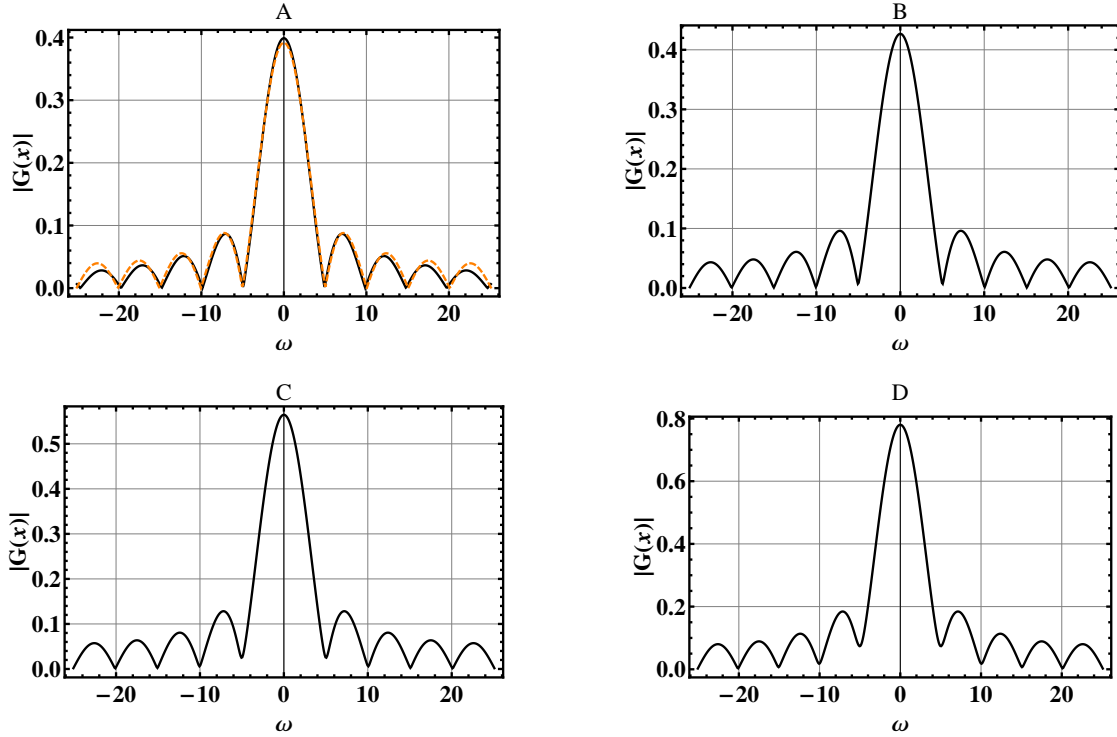


Figure 8: Fractional Fourier transform as given in (11) for the rectangle function  $\text{rect}(t)$ , computed with  $N = 512$ . We plot in **A** the exact Fourier transform (solid line) against the XFT (dashed line). In this case we have  $\varphi = \pi/2$ . In the cases **B**, **C** and **D**, the argument  $\varphi$  is 1, 1/2 and 1/4 respectively. Note that the spectrum peaks becomes greater as the argument  $\varphi$  decreases.

## 4 Conclusions

As it is known, there are not universal methods. Some points for and against the fast algorithm to compute the fractional Fourier transform presented in this paper have to be noticed. First, note that the XFT and their inverse have simple forms given by explicit matrix elements that can be computed easily for complex values of the parameter  $z = r \exp(i\varphi)$  lying inside the unitary circle, not only on the boundary. On the other hand, the XFT can be interpreted as a complex-windowed FFT, as fast as the latter and certainly,

it is an improvement of the FFT since it performs pretty well even with singular functions or non-periodic functions and detects the well-known integer-harmonic spectrum as the FFT does. Besides, it is able to detect half-integer harmonic frequencies with no leakage. However, the convergence of the XFT to the fractional Fourier transform can be assured only if the function to be transformed satisfies the quadrature formula (12). Besides, the XFT also presents some pitfalls and artifacts as the FFT: it presents leakage for some sinusoidal signals and yields spurious frequencies if the input signal has very high frequencies and the number of samples is small.

## References

- [1] V. Namias, *The Fractional Order Fourier Transform and its Application to Quantum Mechanics*, J. Inst. Maths. Applics. **25** (1980) 241-265.
- [2] H.M Ozaktas, Z. Zalevsky, M.A. Kutay, *The Fractional Fourier Transform with Applications in Optics and Signal Processing*, John Wiley and Sons, Chichester, UK, 2001.
- [3] N. Wiener, *Hermitian polynomials and Fourier analysis*, J. Math. and Phys. MIT **8** (1929) 70-73.
- [4] K.B Wolf, *Integral Transforms in Science and Engineering*, Ch. 9-10, Plenum Press, New York, 1979.
- [5] M. Moshinsky and C. Quesne, *Linear Canonical Transformations and their unitary representations*, J. Math. Phys., **12** (1971), 1772-1783.
- [6] H.M. Ozaktas, O. Ankan, M.A. Kutay and G. Bozdağı, *Digital Computation of the Fractional Fourier Transform*, IEEE Trans. Signal Processing, **44** (1996) 2141-2150.
- [7] R. Saxena and K. Singh, *Fractional Fourier transform: A novel tool for signal processing*, J. Indian Inst. Sci. **85** (2005) 11-26.
- [8] P.J. Oonincx, *Joint timefrequency offset detection using the fractional Fourier transform*, Signal Processing **88** (2008) 2936-2942.
- [9] K.K. Sharma, S.D. Joshi, *Time delay estimation using fractional Fourier transform*, Signal Processing **87** (2007) 853-865.
- [10] L. Onural, H.M. Ozaktas, *Signal processing issues in diffraction and holographic 3DTV*, Signal Processing: Image Communication **22** (2007) 169-177.
- [11] C. Vijaya, J.S. Bhat, *Signal compression using discrete fractional Fourier transform and set partitioning in hierarchical tree*, Signal Processing **86** (2006) 1976-1983.



- [12] G. Gonon, O. Richoux and C. Depollier, *Acoustic wave propagation in a 1-D lattice: analysis of nonlinear effects by the fractional Fourier transform method*, Signal Processing **83** (2003) 2469–2480.
- [13] T. Alieva and A. Barbé, *Fractional Fourier and Radon-Wigner transforms of periodic signals*, Signal Processing **69** (1998) 183-189.
- [14] R. G. Campos, and L.Z. Juárez, *A discretization of the Continuous Fourier Transform*, Il Nuovo Cimento **107B** (1992) pp. 703-711.
- [15] R. G. Campos, *A Quadrature Formula for the Hankel Transform*, Numerical Algorithms, **9** (1995) pp. 343-354
- [16] R. G. Campos, F. Domínguez Mota and E. Coronado, *Quadrature formulas for integrals transforms generated by orthogonal polynomials*, <http://arxiv.org/abs/0805.2111v1> [math.NA].
- [17] B.M. Hennelly and J.T. Sheridan, *Fast Numerical Algorithm for the Linear Canonical Transform*, J. Opt. Soc. Am, **A22** (2005), 928-937.
- [18] J.J. Heally and J.T. Sheridan, *Sampling and discretization of the linear canonical transform*, Signal Processing, **82** (2009) 641-648.
- [19] Szegő G., *Orthogonal Polynomials*, Colloquium Publications, American Mathematical Society, Providence, Rhode Island, 1975.
- [20] G. H. Golub y J. H. Welsch, *Calculation of Gauss quadrature rules*, Math. Comp. **23** (1969) 221-230.
- [21] W. Gautschi, *Orthogonal polynomials and quadrature*, Electron. Trans. Numer. Anal. **9** (1999) 65-76.
- [22] A. Erdélyi (ed.), *Higher Transcendental Functions*, Vols I and II, McGraw Hill, New York, 1953.
- [23] P. Pellat-Finet and E. Fogret, *Complex order fractional Fourier transforms and their use in diffraction theory. Application to optical resonators*, Optics Comm. **258** (2006) 103-113.
- [24] S. Solís-Ortíz, R.G. Campos, J. Félix and O. Obregón, *Coincident frequencies and relative phases among brain activity and hormonal signals*, Behav. Brain Funct. 2009, **5**:18 doi:10.1186/1744-9081-5-18
- [25] A. Erdélyi (ed.), *Tables of Integral Transforms*, Vol 1, McGraw Hill, New York, 1953.
- [26] F. Oberhettinger, *Fourier Expansions, a Collection of Formulas*, Academic Press, New York, USA, 1973